The microwave heating systems at the WEGA stellarator - status and prospects

M.Schubert, G.B.Warr, Y.Podoba, H.P.Laqua, W.Kasparek[1], E.Holzhauer[1], D.Keil

Max-Planck-Institut für Plasmaphysik, EURATOM Association, Greifswald, Germany

[1] *Institut für Plasmaforschung, Universität Stuttgart, Germany*

1 Introduction

The WEGA is a classical l=2, m=5 stellarator, operating at the Greifswald branch of IPP. Its main uses are educational training, testing continuous operation of technical infrastructure, and evaluation of new diagnostic equipment. The machine and its main parameters are displayed schematically in Figure 1. WEGA also has a set of vertical field coils that are not shown in the Figure. Steady state plasmas are produced in H, He, and Ar, using two magnetron sources operating at 2.45 GHz.

First harmonic obliquely launched ordinary (O) mode heating in WEGA produces bulk plasma densities above the O-mode cut-off density [1]. A scheme via OXB mode conversion [2] has been proposed to explain the heating mechanism, as the resonant region is inaccessible to the O-mode [3].

Plasma heating via this mode conversion process has been successfully demonstrated on W7-AS [4]. The inverse process has also been used as an ECE diagnostic of overdense plasmas [5]. These investigations, however, are based on the condition $\lambda \ll L_n$, $L_n = n_e/\nabla_r n_e$, which is not fulfilled at the WEGA, since $\lambda \approx 12\,\mathrm{cm}$ is of the same order as the small radius of the vacuum vessel $a = 19\,\mathrm{cm}$.

This paper presents the results of a full wave field simulation of the O-SX process (SX: slow extraordinary mode) in 2D geometry with $\lambda = \mathcal{O}(L_n)$. The subsequent SX-B

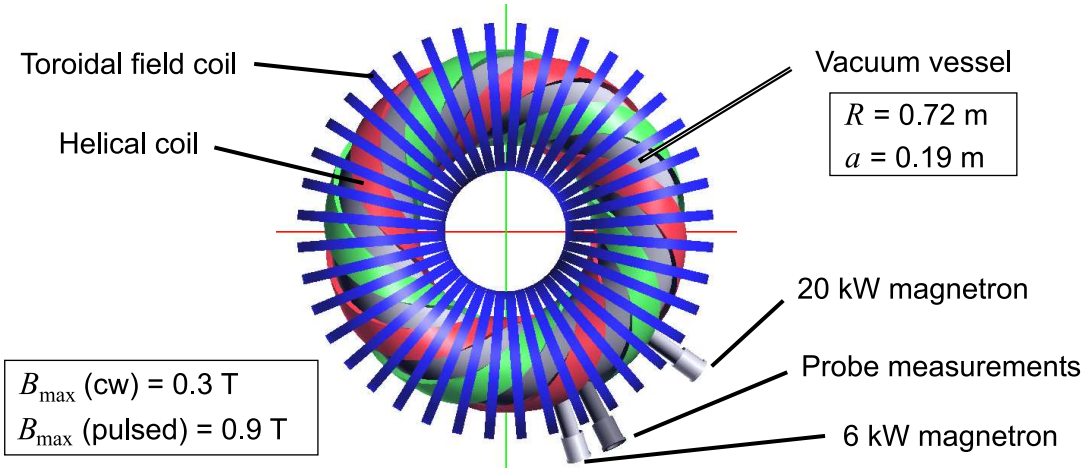

Figure 1: *Top view of the WEGA machine, displaying the toroidal vacuum vessel (grey), and two coil systems. Also indicated are the ports for launching the microwave heating power and for doing probe measurements.*

conversion yields a resonant increment of the wave's amplitude, localised at the upper hybrid resonance (UHR). Langmuir and high-frequency probe measurements have been carried out inside the conversion layer at WEGA. The probe measurements verify the localised amplitude increment and are thus in agreement with the simulations of the conversion process.

A 28 GHz system is being installed for central heating of the WEGA plasma. An outline of the proposed X2 and OXB heating schemes is given.

2 Full wave field simulation

We consider a finite 2D slab geometry, with a homogeneous magnetic field in the z direction and a density gradient in x direction. The density increases linearly from zero at $x=0$ to approximately twice the O-mode cut-off density at $x=20\,\mathrm{cm}$. An O-mode wave ($\lambda_{\mathrm{vacuum}}=12\,\mathrm{cm}$) is launched obliquely from the lower boundary. Maxwell's equations

$$\nabla\times\vec{E}=-\frac{1}{c}\frac{\partial\vec{B}}{\partial t}\quad\text{and}\quad\nabla\times\vec{B}=\frac{1}{c}\frac{\partial\vec{E}}{\partial t}+\frac{4\pi}{c}\vec{j}\qquad[cgs]$$

are solved on the rectangular grid using a Finite-Difference Time-Domain method. The grid has typically between 300 and 700 points for one vacuum wavelength. Following [6], the plasma response is included in the current density $\vec{j}$, which is related to the electric field via the cold dielectric tensor $\overleftrightarrow{\chi}$:

$$\vec{j}=-i\omega\epsilon_0\overleftrightarrow{\chi}\vec{E}\ ,\qquad\overleftrightarrow{\chi}=\frac{-\omega_{pe}^2}{\omega^2-\omega_{ce}^2}\begin{pmatrix}1 & -i\,\omega^{-1}\omega_{ce} & 0\\ i\,\omega^{-1}\omega_{ce} & 1 & 0\\ 0 & 0 & 1-\omega^{-2}\omega_{ce}^2\end{pmatrix}.$$

At the boundary of the simulation area, absorption is applied by multiplying the electric field values with a damping factor. Only the O-SX conversion at the O-mode cut-off and the SX propagation towards the UHR are simulated. Displaying the Bernstein (B) mode would require a simulation of the hot plasma (non-zero Larmor radii of the electrons), at the expense of computing time. Instead, the SX-B mode conversion at the UHR is replaced in the simulation by an artificial damping, which is achieved by choosing the damping coefficient proportional to k^2, i.e. the second spatial derivative of the electric field. Since k diverges near the UHR, this acts as a drain of the SX wave energy. A snapshot of the electric field component E_x is shown in Figure 2 on the left, and compared to the ray tracing representation of the OXB process.

3 Setup and results of the probe measurements

A reciprocating probe system was installed near the launch of the 2.45 GHz radiation (see figure 1). The probe system incorporates bent 3-pin probes (figure 3) to measure the electric field amplitude of the 2.45 GHz radiation, and several Langmuir probes to determine the plasma electron density.

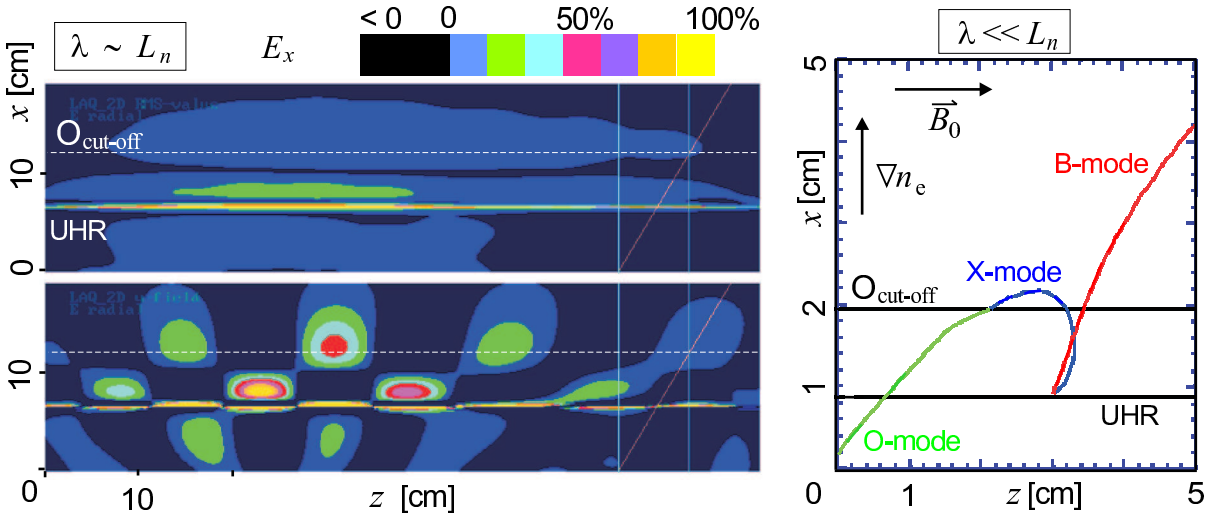

Figure 2: *Comparison of the full wave calculation of the O-SX mode conversion with OXB ray tracing [4]. Different scale lengths are used. Left: Upper half is the time average of the x component of the electric field intensity E_x. The lower half is a snapshot of the E_x amplitude, displaying positive values only. Right: The ray trace path of the obliquely launched wave.*

The design of the 3-pin probe is optimised to resolve the mm-scale resonant increase of the radial electric field component near the UHR. The signal is mixed down to 100 MHz in a microwave circuit and recorded by a fast sampling (1 GHz) oscilloscope. Plasma electron density measured by the Langmuir probes is used to determine the location of the UHR.

Profiles of the 3-pin probe signal are recorded in the boundary plasma of WEGA. A localised maximum of the averaged electric field strength is visible (Figure 4, left). Since the probe shaft can be rotated by 180° around the reciprocation axis, different probe orientations, i.e. towards and away from the 2.45 GHz launch are possible. It is observed that the signal quality depends on the orientation, a fact that is not yet completely understood.

Several plasma discharges in Ar were performed, varying the magnetic configuration,

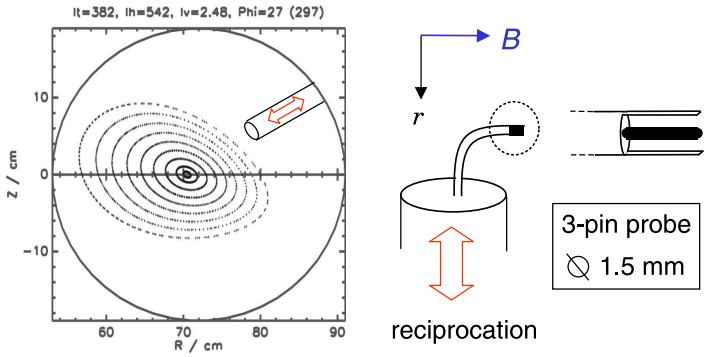

Figure 3: *Schematic of the probe measurement system. On the left a cross section of WEGA's magnetic surfaces at $\iota/2\pi \approx 0.2$ is shown, together with the radial movement of the probe system. On the right the 3-pin probe is shown in a vertical view. The 3-pin probe consists of a central detection pin and two flanking pins, which are electrically connected to the coaxial shielding. The tip tube is bent at 90° relative to the reciprocation axis.*

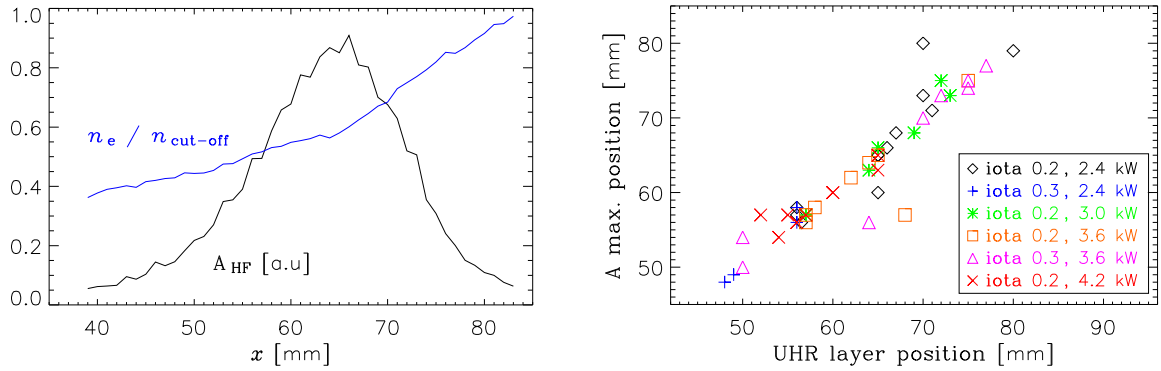

Figure 4: *Results of probe measurements in WEGA. On the left: Amplitude of the 3-pin probe signal as a function of probe position. Overplotted is the plasma electron density, normalised to the O-mode cut-off. On the right: Correlation plot of the location of the maximum in the 3-pin probe signal, and the location of the UHR. Different colours correspond to different magnetic configurations and different heating power.*

the plasma heating, and the vertical field. The variation yields different locations of the UHR. The location of the maximum in the 3-pin probe signal follows the location of the UHR (Figure 4, right).

4 Discussion and Outlook

The rise of the wave field amplitude E_r near the UHR is predicted by the full wave field simulation of the O-SX conversion process, and is confirmed by the probe measurements. Evidence in favour of heating via O-SX-B mode conversion is also provided by the fact that oblique launch of the O-mode in WEGA yields highest plasma densities [1]. The efficiency of O-SX estimated using the ray tracing approximation is 20% [3]. This is of the same order as the heating efficiency estimated from the kinetic energy content in the WEGA plasma [7]. The calculation of the O-SX efficiency is currently being determined using the results of the full wave simulation. Loop probes are being installed to measure profiles of the magnetic component of the wave.

5 WEGA 28 GHz ECRH System

A 28 GHz ECRH System using a 20 kW CPI Gyrotron is currently being installed on WEGA. As shown in Figure 5, it will initially be configured for second harmonic extraordinary (X2) mode heating of the plasma. Using ISS95 [8], average electron temperatures $\langle T_e \rangle = 50$ eV and electron densities $n_e < 5 \times 10^{18}$ m^{-3} are expected. The system will be used to generate supra-thermal particles for fast particle confinement studies in different magnetic configurations (various ι) in the stellarator geometry. It can also be used for such studies in stellarator-tokamak hybrids, when the power supply for the WEGA transformer coils is installed.

The ECRH system has been designed with potential future use for overdense OXB mode heating of the WEGA plasma in mind, where an oblique launch arrangement is

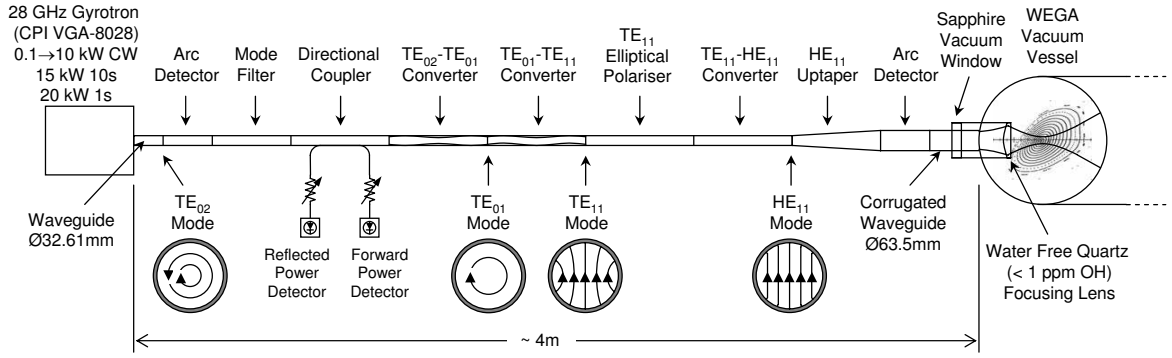

Figure 5: *Schematic layout of the 28 GHz ECRH plasma heating system for WEGA. Layout and design of new waveguide components by IPF Stuttgart. Vacuum window and waveguide components kindly loaned by CIEMAT Madrid. New waveguide components manufactured at IPP Greifswald.*

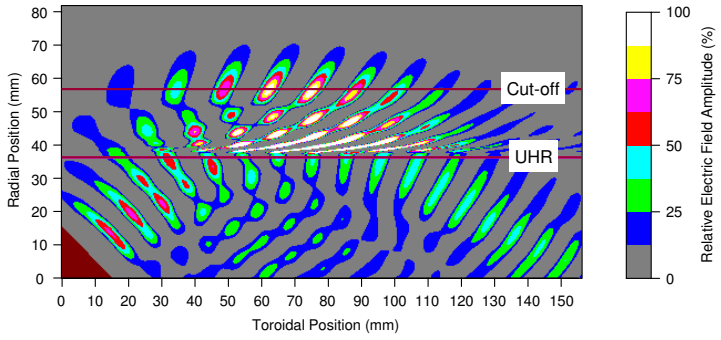

Figure 6: *Time snapshot of the full wave calculation of the O-SX mode conversion for oblique launch of 28 GHz radiation into the WEGA plasma. Density increases linearly with radial position, magnetic field is parallel to the toroidal axis and, for clarity, only the positive electric field wave amplitude is shown. O mode radiation is launched bottom left at 45° incidence to the plasma, reflects off the cut-off layer, and is partially converted into the X mode. The X mode radiation is unable to propagate back through the upper hybrid resonance (UHR) layer, giving rise to an electrostatic Bernstein wave (not shown), which in turn transfers power through the cutoff layer and into the centre of the plasma. The remaining reflected O mode radiation propagates through the UHR layer to the bottom right.*

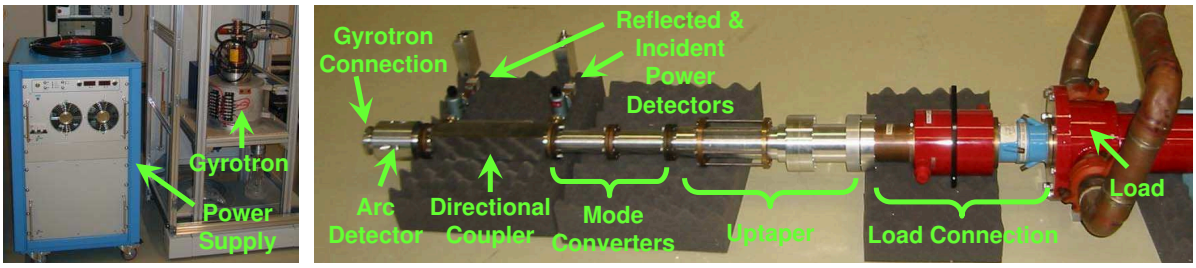

Figure 7: *Left: CPI Gyrotron with IPF Stuttgart power supply. Right: Transmission line assembly for the gyrotron load tests. Load and adaptor components kindly loaned by CIEMAT Madrid. New components designed by IPF Stuttgart and manufactured at IPP Greifswald.*

required. Here, using ISS95, average electron temperatures $\langle T_e \rangle = 25$ eV and electron densities $n_e > 10^{19}$ m^{-3} are anticipated. This is ideal for wave physics studies and to test W7-X divertor diagnostics. Results of computed OX mode conversion of the 28 GHz

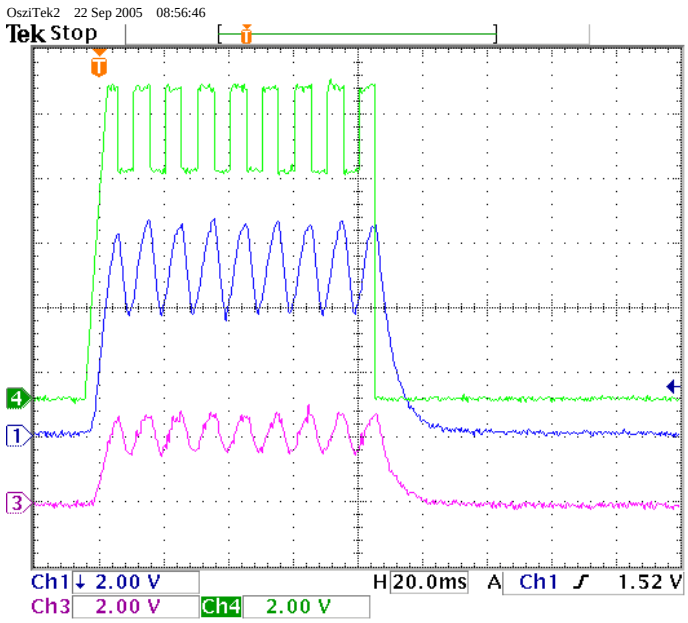

Figure 8: *Gyrotron power supply full power modulation test results. Shown are the input voltage control signal, Ch4, and the measured output voltage, Ch1, and current, Ch3, across a large 2.77 Ω resistor. For Ch1, each division corresponds to 10 kV, while for Ch3 each division corresponds to 0.72 A. The 24 to 34 kV output voltage from the power supply corresponds to 0.1 to 20 kW power output from the Gyrotron.*

radiation in WEGA are shown in Figure 6.

The gyrotron power supply has been successfully tested and integrated into the WEGA control system. Results from power modulation tests are shown in Figure 8. Gyrotron load tests are about to commence. Photographs of the Gyrotron, its power supply and of the transmission line assembly for the load test are given in Figure 7. The final components for the plasma heating transmission line are about to be manufactured. First 28 GHz ECRH plasmas in WEGA are anticipated in early 2006.

Acknowledgements

We are grateful to CIEMAT Madrid for the loan of transmission line components and to IPF Stuttgart for the design of new transmission line components.

[1] J. Lingertat *et al.*, in *30th EPS Conference on Controlled Fusion and Plasma Physics (St Petersburg)*, edited by R. Koch and S. Lebedev (The European Physical Society, 2003), Vol. 27A, P–1.10.

[2] J. Preinhalter and Kopecký, J.Plasma Physics **10**, 1 (1973).

[3] Y. Podoba *et al.*, in *14th Intern. Conf. on Stellarators* (IPP, Greifswald, 2003).

[4] H. Laqua *et al.*, Physical Review Letters **78**, 3467 (1997).

[5] F. Volpe, H. Laqua, and W7-AS Team, Rev. Scientific Instr. **74**, 1409 (2003).

[6] A. Ram and S. Schultz, Physics of Plasmas **7**, 4084 (2000).

[7] K. Horvath, PhD Thesis, Ernst-Moritz-Arndt-Universität Greifswald, 2004.

[8] U. Stroth *et al.*, Nuclear Fusion **36**, 1063 (1996).